off-diagonal element for the second hydrogen atom, in the limit of small hydrogen polarization (diagonal elements approximately equal):

$$(\rho_H^{ff})_{21} = \rho_{21}^{i} - \tfrac{1}{4}(1-\cos\Delta)[\tfrac{3}{2}\rho_{21}^{i} - \tfrac{1}{2}\mathrm{Re}\{\bar{e}_T\} - \tfrac{1}{2}\mathrm{Re}\{\bar{g}_T\}]$$

$$+\tfrac{1}{4}i(1-\cos\Delta)[\tfrac{1}{2}\mathrm{Im}\{\bar{e}_T\} + \tfrac{1}{2}\mathrm{Im}\{\bar{g}_T\}]\,. \qquad (7)$$

The imaginary terms in Eq. (7) represent a frequency shift which does *not* reverse with polarization. They are proportional to $(1-\cos\Delta)^2$ and represent spin coordinates which effectively left the first hydrogen atom to ride with the tritium atom until second collision, after which they contribute to the hydrogen resonance. These terms depend on the frequency difference between the isotopes and amount to averaging the frequencies of several transitions in the sample.[7(a),7(b)]

Much more complicated situations can arise, especially when lines in neighboring atoms are not completely resolved. In such a case, accidental coincidences between multiple quantum transitions can also contribute to the spin-exchange shifts. The case of Rb and H isotopes provide a variety of such coincidences. Additional shifts also occur in the case of double resonance.[9]

In conclusion, the predictions of a single-collision model do not include many experimentally realized conditions. One must expect to find frequency shifts which do not reverse with polarization and shift-to-broadening ratios which are not constant.

*Research sponsored by the U. S. Air Force Office of Scientific Research, Air Force Systems Command, under AFOSR Grant No. 249-67.

[1]P. L. Bender, Phys. Rev. 132, 2154 (1963).

[2]L. C. Balling, R. J. Hanson, and F. M. Pipkin, Phys. Rev. 133, A607 (1964).

[3]S. B. Crampton, Phys. Rev. 158, 57 (1967); D. Kleppner, H. D. Berg, S. B. Crampton, N. F. Ramsey, R. F. C. Vessot, H. E. Peters, and J. Vanier, *ibid.* 138, A972 (1965).

[4]For a recent review see F. G. Major, in *Methods of Experimental Physics*, edited by B. Bederson and W. L. Fite (Academic, New York, 1968), Vol. 7, Pt. B. p. 1.

[5]L. C. Balling, Phys. Rev. 151, 1 (1966).

[6]E. S. Ensberg and C. L. Morgan, in *Proceedings of the International Conference on Precision Measurement and Fundamental Constants*, edited by D. N. Langenberg and B. N. Taylor, NBS Special Publication 343 (U. S. GPO, Washington, D. C., 1971).

[7]Special cases of coherence transfer are discussed in (a) L. D. Schearer, F. D. Colegrove, and G. K. Walters, Rev. Sci. Instr. 35, 767 (1964). (b) H. G. Dehmelt, *ibid.* 35, 768 (1964). (c) G. A. Ruff and T. R. Carver, Phys. Rev. Letters 15, 282 (1965). (d) G. W. Series, Proc. Phys. Soc. (London) 90, 1179 (1967).

[8]M. A. Giochon, J. E. Blamont, and J. Brossel, Compt. Rend. 243, 1859 (1956). For a recent review see G. zu Putlitz, *Atomic Physics*, edited by B. Bederson, V. W. Cohen, and F. Pichanick (Plenum, New York, 1969), p. 227.

[9]Double resonance is a common technique for measuring the magnetic field in the H maser. See D. Kleppner *et al.*, Ref. 3.

PHYSICAL REVIEW A VOLUME 3, NUMBER 6 JUNE 1971

Theory of the Liquid-Solid Phase Transition

T. Schneider
IBM Zurich Research Laboratory, 8803 *Rüschlikon, Switzerland*
(Received 23 December 1970)

We reanalyze in greater generality the recently predicted phenomena associated with the liquid-solid phase transition.

Recently,[1] the density response of a fluid has been investigated with particular emphasis on those fluctuations which may be considered as precursors to freezing. Neglecting the instabilities against nucleation and growth of small crystallites, a definite stability limit has been found at which the supercooled liquid as a whole becomes intrinsically unstable with respect to a density fluctuation of wave number Q_0. Q_0 is the position of the first maximum in the structure factor $S(Q)$ and corresponds to the lattice vector of the solid into which the liquid freezes.

It is the purpose of this note to show that the stability limit of the liquid and the associated phenomena may be derived in greater generality, and therefore, that the predictions of Ref. 1 are more general than the approximations suggest.

In doing so we write the free energy F of the fluid in a static applied potential $V_{ex}(r)$ in the form

$$F[n] = \int V_{ex}(\vec{r})\, n(\vec{r})\, d^3r + F_s[n] + \tfrac{1}{2}\int\int V(|\vec{r}-\vec{r}'|) n(\vec{r}) n(\vec{r}')\, d^3r\, d^3r' + F_c[n]. \qquad (1)$$

$F_s[n]$ is the free energy of noninteracting particles with density $n(r)$ at pressure p and temperature

T. By definition $F_c[n]$ is the correlation contribution to the free energy, and the third term represents the Hartree interaction. It has been shown[2] that $F[n]$ assumes its minimum value for the correct density $n(r)$. In order to apply this minimum principle, we write the applied potential in the form

$$V_{ex}(r) = \frac{1}{2} \sum_{\vec{Q} \neq 0} [V_{ex}(\vec{Q})\, e^{i\vec{Q}\cdot\vec{r}} + \text{c. c.}]. \tag{2}$$

The density of the system will then contain a linear response and may be written as

$$n(\vec{r}) = \bar{n} + \delta n(\vec{r}) = \bar{n} + \frac{1}{2} \sum_{\vec{Q} \neq 0} [n(\vec{Q})\, e^{i\vec{Q}\cdot\vec{r}} + \text{c. c.}]\ ; \tag{3}$$

$\bar{n}$ is the mean density and $n(\vec{Q})$ denotes the density fluctuations. Furthermore, we expand $F_s[n]$ and $F_c[n]$ in a functional Taylor series:

$$F_c[n] = F_c[\bar{n}] + \tfrac{1}{2}\bar{n}^2 \int F_c^{(2)}(|\vec{r} - \vec{r}\,'|, [\bar{n}])\, \delta n(\vec{r})\, \delta n(\vec{r}\,')\, d^3r\, d^3r'\ , \tag{4}$$

where

$$F_c^{(2)}(|\vec{r} - \vec{r}\,'|, [\bar{n}]) = \left. \frac{\delta^2 F_c[n]}{\delta n(\vec{r})\, \delta n(\vec{r}\,')} \right|_{\bar{n}}\ . \tag{5}$$

Using Eqs. (1)–(5), $F[\bar{n}]$ may be rewritten in the form

$$F[n] = F[\bar{n}] + \sum_{\vec{Q} \neq 0} \frac{1}{2} \{ [V_{ex}(\vec{Q}) n^*(\vec{Q}) + \text{c. c.}]\, \bar{n}^{-1} + [F_s^{(2)}(Q, [\bar{n}]) + (1/\bar{n}^2)\ V(Q) + F_c^{(2)}(Q, [\bar{n}])]\, n(\vec{Q}) n^*(\vec{Q}) \}. \tag{6}$$

Recalling that[3]

$$N F_s(n) = -V[nk_BT \ln(1/n) + nf(T)], \tag{7}$$

we find

$$F_s^{(2)}(Q, [\bar{n}]) = \frac{1}{N} \left. \frac{d^2 N F_s(n)}{dn^2} \right|_{\bar{n}} = \frac{k_B T}{\bar{n}^2}\ . \tag{8}$$

Now we use the fact that $F[n]$ assumes its minimum for the correct density. Hence, we have

$$\frac{\partial F[\bar{n}]}{\partial n^*(\vec{Q})} = \frac{\partial F[n]}{\partial n(\vec{Q})} = 0\ , \tag{9}$$

$$\frac{\partial^2 F[n]}{\partial n^*(\vec{Q})\ \partial n(\vec{Q})} > 0\ . \tag{10}$$

Performing these differentiations in Eq. (6) and substituting Eq. (8) we obtain

$$n(\vec{Q})/\bar{n} = \chi(Q, [\bar{n}])\, V_{ex}(\vec{Q}), \tag{11}$$

where

$$-\chi(Q, [\bar{n}]) = 1/[k_BT + V_{eff}(Q, [\bar{n}])]\ , \tag{12}$$

$$V_{eff}(Q, [\bar{n}]) \equiv V(Q) + \bar{n}^2 F_c^{(2)}(Q, [n]), \tag{13}$$

$$-1/\chi(Q, [\bar{n}]) > 0. \tag{14}$$

$\chi(Q) \equiv \chi(Q,\ \omega = 0)$ is the static density response function. The condition (14) ensures that the free energy is minimal, or in other words, that the system is in an equilibrium state either absolutely stable or metastable. Obviously, unstable states of the system are those for which

$$-1/\chi(Q, [\bar{n}]) \leq 0\ . \tag{15}$$

Therefore,

$$-1/\chi(Q, [\bar{n}]) = 0 \tag{16}$$

determines the stability limit of the fluid (Q_L, P_L, T_L).

In the special case of $Q_L = 0$, the stability condition goes over into the familiar result

$$-\frac{1}{\chi(0, [\bar{n}])} = \frac{1}{\bar{n}\kappa_T} = \left(\frac{\partial P}{\partial \bar{n}}\right)_T = 0\ . \tag{17}$$

Here κ_T is the isothermal compressibility, and P the pressure. In deriving Eq. (17) we used the compressibility sum rule. It is now evident that the end point of an isotherm (point b in Fig. 1) in the p-$\bar{n}$ diagram is determined by the stability limit [Eq. (16)], with either $Q_L = 0$ or $Q_L \neq 0$.

Our next concern is to relate the density response function and the stability limit to specific properties of the system. To this end we recall the following form of the fluctuation-dissipation theorem for classical systems[4]:

$$-\chi(Q, [\bar{n}]) = (1/k_BT) S(Q). \tag{18}$$

The structure factor $S(Q)$ is the Fourier transform of the static pair correlation function $g(r)$,

$$S(Q) - 1 = \bar{n} \int d^3r\, e^{i\vec{Q}\cdot\vec{r}} [g(r) - 1]\ . \tag{19}$$

Combining Eqs. (12), (16), and (18), the stability condition now becomes

$$-1/\chi(Q, [\bar{n}]) = k_BT/S(Q) = k_BT + V_{eff}(Q, [\bar{n}]) = 0\ . \tag{20}$$

The same result has been derived in Ref. 1, using a generalized random-phase approximation. The weak point of this approach is the neglect of damping mechanisms other than Landau damping. The present derivation is based on a generalized minimum principle for the free energy. Two-body forces are assumed, and higher than bilinear terms in the functional Taylor expansion are neglected. This neglect is equivalent to the assumption that the response is linear. Hence, we come to the conclusion that the stability condition holds more generally than the original approximations of Ref. 1 suggest.

The stability condition, which determines the stability limit $(\bar{n}_L, Q_L; T_L, Q_L, P_L)$, implies that the mean density fluctuation $S(Q)$ with the particular wave number Q_L increases as this limit is approached. The experimental structure factor data, taken in the stable region of the liquid phase, show that

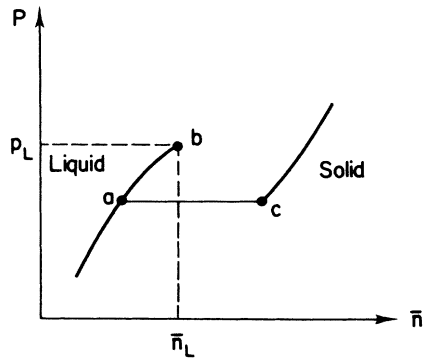

FIG. 1. Schematic graph of an isotherm of the liquid-solid phases. a, c are the coexistence points determined by $\mu_{\text{liquid}} = \mu_{\text{solid}}$. b denotes the endpoint of the liquid-phase isotherm determined by the stability condition [Eq. (16)]. Along {a, b} the liquid is metastable.

$S(Q)$ is dominated by a large peak at a value Q_0.[5,6] Furthermore, it is known that $S(Q_0)$ increases under applied pressure[6] and decreasing temperature.[5] These facts permit two important conclusions. First, the large mean density fluctuations associated with the stability limit of the liquid phase are already present in the stable region. Second, the instability occurs at a value $Q_L = Q_0$, which corresponds to the reciprocal lattice vector of the solid into which the liquid freezes. In fact, as one expects, the Q value at which the instability occurs influences the nature of the state on the other side of the stability limit, or in other words, corresponds to the wave vector of the permanent density fluctuations in the solid.

Near the stability limit only the region $Q \approx Q_L$ is important. Thus, using Eq. (20) and setting

$$(1/k_BT)V_{\text{eff}}(Q) = -1 + A(T - T_L) + B(Q - Q_L)^2, \tag{21}$$

we may write for $\bar{n} = \text{const}$

$$S(Q) = \frac{1}{A(T - T_L)} \frac{1/\xi^2}{1/\xi^2 + (Q - Q_L)^2}, \tag{22}$$

where

$$\xi^2 = B/A(T - T_L). \tag{23}$$

We observe that $S(Q)$ increases at Q values $Q \approx Q_L$ and that the width of the peak becomes smaller as we approach the stability limit. A precursor of this critical behavior has been observed in liquid lead.[5] Clearly, this effect would be more dramatic in an experiment performed on the metastable (supercooled) liquid.

Finally, we consider the dynamic aspects associated with the stability limit. Following Kadanoff and Martin[7] we recall that the dynamic form factor $S(Q, \omega)$ can always be written in the form

$$S(Q,\omega) = \frac{k_BT}{\pi m}\left\{Q^4\Lambda(Q,\omega)\Big/\left[\left(\omega^2 - \frac{k_BTQ^2}{mS(Q)} - Q^2\omega P\int_{-\infty}^{+\infty}\frac{d\omega'}{\pi}\frac{\Lambda(Q,\omega')}{\omega - \omega'}\right)^2 + [Q^2\omega\Lambda(Q,\omega)]^2\right]\right\}. \tag{24}$$

$\Lambda(Q, \omega)$ is an unknown function, which may be interpreted as having frequency-dependent and wave-number–dependent transport coefficients. This suggests that the details of the dynamics are hidden in the unknown function $\Lambda(Q, \omega)$. However, one expects that $\Lambda(Q, \omega)$ is a smooth function of Q and ω.[7]

Our thermodynamic approach revealed that the dynamic instability occurs at $\omega = 0$. In the small-ω region we may rewrite $S(Q, \omega)$ [Eq. (24)] in the form

$$S(Q,\omega) = \frac{k_BT}{\pi m}\frac{1/\Lambda(Q,0)}{\Gamma^2(Q) + \omega^2}, \tag{25}$$

where

$$\Gamma^2(Q) = \left(\frac{k_BT}{m\Lambda(Q,0)S(Q)}\right)^2 = \left[\frac{k_BT}{m\Lambda(Q,0)}\left(1 + \frac{V_{\text{eff}}(Q,[\bar{n}])}{k_BT}\right)\right]^2. \tag{26}$$

Using Eqs. (21) and (26) for conditions close to the stability limit we obtain

$$\Gamma^2(Q) = \left(\frac{k_BT}{m\Lambda(Q,0)}\left[A(T - T_L) + B(Q - Q_0)^2\right]\right)^2. \tag{27}$$

From experiments[5] taken in the stable region it is known that $\Lambda(Q_0, 0)$ is a smooth function of temperature. Hence, in agreement with Refs. 1 and 8 we come to the conclusion that the quasielastic peak becomes narrow as the stability limit is approached. However, the present derivation arrives at this conclusion from appreciably more general assumptions. We only assume that $\Lambda(Q_0, 0)$ is a smooth function of temperature, in agreement with experiment.[5]

The phenomenon of linewidth narrowing of the quasielastic peak at Q_0 is known as the deGennes narrowing,[9] and has been observed by neutron scattering.[5,10] Equations (26) and (27) imply that the deGennes narrowing at Q_0 and its pressure and temperature[5,10] dependence are caused by critical fluctuations associated with the stability limit of the liquid phase. Obviously, as mentioned in the context of the static critical fluctuations [Eq. (23)], the narrowing would be far more drastic in an experiment performed on the metastable (supercooled) liquid.

Finally, we remark that a quantum-mechanical version of the method outlined in this note should

shed additional light onto the phenomena associated with the ^{3}He and the ^{4}He liquid-solid transition. We hope to revert to this problem in subsequent work.

We are indebted to Dr. E. O. Schulz-DuBois for a critical reading of the manuscript and acknowledge fruitful discussions with Professor C. P. Enz, Professor H. Thomas, and Dr. E. Stoll.

[1]T. Schneider, R. Brout, H. Thomas, and J. Feder, Phys. Rev. Letters 25, 1423 (1970).
[2]N. D. Mermin, Phys. Rev. 137, A1441 (1965).
[3]L. D. Landau and E. M. Lifshitz, *Statistical Physics* (Pergamon, London, 1958), p. 121.
[4]D. Pines and P. Nozières, *The Theory of Quantum Liquids* (Benjamin, New York, 1966).
[5]P. A. Egelstaff, Advan. Phys. 16, 147 (1967).
[6]D. G. Henshaw, Phys. Rev. 119, 14 (1960).
[7]L. Kadanoff and P. C. Martin, Ann. Phys. (N. Y.) 24, 419 (1967).
[8]K. K. Kobayashi, J. Phys. Soc. Japan 27, 1116 (1969).
[9]P. G. deGennes, Physica 25, 825 (1959).
[10]B. A. Dasannacharaya and K. R. Rao, Phys. Rev. 137, A417 (1965).

PHYSICAL REVIEW A VOLUME 3, NUMBER 6 JUNE 1971

Tunable Far-Infrared Radiation Generated from the Difference Frequency between Two Ruby Lasers

D. W. Faries,* P. L. Richards, Y. R. Shen, and K. H. Yang
Department of Physics, University of California, Berkeley, California 94720
and
Inorganic Materials Research Division, Lawrence Radiation Laboratory, Berkeley, California 94720
(Received 30 November 1970)

Far-infrared radiation generated from the difference frequency between two temperature-tuned ruby lasers operated on the R_1 and R_2 transitions has been observed. This radiation is continuously tunable over the frequency range 20–38 cm^{-1}. Lithium niobate was used as a mixing crystal. The expected frequencies of the far-infrared radiation were measured using a Fabry-Perot interferometer. The phase-matching conditions were also verified.

In a previous paper, we described the generation of tunable far-infrared radiation over the frequency range 1.5–8.1 cm^{-1} by beating two temperature-tuned ruby laser beams in a nonlinear crystal.[1] By operating one laser on the R_1 transition and the other on the R_2 transition, we have now obtained tunable radiation in the range 20–38 cm^{-1}. In order to produce laser action on the R_2 transition,[2–4] we used essentially a Lyot-Ohman[5,6] filter in the laser cavity to discriminate against the R_1 transition.[7] The power output of the R_2 laser was about $\frac{1}{2}$ MW, compared with the 1-MW output of the R_1 laser. Lithium niobate was used for the nonlinear crystal. The additional experimental apparatus and the measurement technique were essentially the same as described earlier.[1]

If both lasers are operated at room temperature, the difference-frequency radiation generated should be at 29 cm^{-1}. In order to phase-match this difference-frequency generation process, a 1.5-mm slice of $LiNbO_3$ was cut with the c axis tilted approximately 18° away from the normal to the surface. The frequency of the far-infrared output was measured using a Fabry-Perot interferometer with electroformed metal mesh mirrors. The measured transmission curve[8] of the Fabry-Perot interferometer is compared in Fig. 1(a) with a theoretical curve calculated for a frequency of 28.8 cm^{-1}. Since the interferometer has a finesse of about 4, the spectral purity of the far-infrared radiation could not be measured. In Fig. 1(b) the Fabry-Perot transmission is shown for radiation generated with the R_1 laser at room temperature and the R_2 laser at −23 °C. The calculated transmission for 35.8 cm^{-1}, the frequency expected from the known temperature dependence of the R_2 transition, is also shown.[9] The same $LiNbO_3$ crystal was used, but it was oriented for phase matching at 35.8 cm^{-1}.

The phase-matching curve for production of the difference frequency at 29 cm^{-1} is shown in Fig. 2. The absorption coefficient for $LiNbO_3$ at 29 cm^{-1} is 18 cm^{-1}.[10] Normalized theoretical curves obtained by solving Maxwell's equations in the plane-wave approximation, with and without absorption,[1,11] are shown for comparison. The effect of absorption changes the width at half-maximum very little, but shows a definite difference at the wings of the curves. The shapes of the curves would not be changed appreciably by including diffraction and